Geol Rundsch (1996) 85:647–661

ORIGINAL PAPER

O. Parlak · M. Delaloye · E. Bíngöl

Mineral chemistry of ultramafic and mafic cumulates as an indicator of the arc-related origin of the Mersín ophiolite (southern Turkey)

Received: 12 December 1995 / Accepted: 15 June 1996

Abstract The Mersin ophiolite, represented by approximately 6-km-thick oceanic lithospheric section on the southern flank of the Taurus calcareous axis, formed in the Mesozoic Neo-Tethyan ocean some time during Late Cretaceous in southern Turkey. The ultramafic and mafic cumulates having over 3 km thickness consist of dunite ± chromite, wehrlite, clinopyroxenite at the bottom and pass into gabbroic cumulates in which leucogabbro, olivine-gabbro and anorthosite are seen. Crystallization order is olivine ($Fo_{91–80}$) ± chromian spinel (Cr# 60–80), clinopyroxene (Mg# $_{95–77}$), plagioclase ($An_{95.6–91.6}$) and orthopyroxene (Mg# $_{68–77}$). Mineral chemistry of ultramafic and mafic cumulates suggest that highly magnesian olivines, clinopyroxenes and absence of plagioclase in the basal ultramafic cumulates are in good agreement with products of high-pressure crystal fractionation of primary basaltic melts beneath an island-arc environment. Major, trace element geochemistry of the cumulative rocks also indicate that Mersin ophiolite was formed in an arc environment. Coexisting Ca-rich plagioclase and Fo-rich olivine in the gabbroic cumulates show arc cumulate gabbro characteristics. Field relations as well as the geochemical data support that Mersin ophiolite formed in a supra-subduction zone tectonic setting in the southern branch of the Neo-Tethys in southern Turkey.

Key words Cumulate · Mineral chemistry · High-pressure fractionation · Suprasubduction

Osman Parlak (✉)[1] · Michel Delaloye
Department of Mineralogy, University of Geneva,
1211 Geneva 4, Switzerland
Fax: +41 22 3205732
e-mail: Parlak@sc2a.unige.ch

Ergüzer Bíngöl
Department of Geology, Çukurova University,
TR-01330 Adana, Turkey

Present address:
[1]Department of Geology, Çukurova University,
TR-01330 Adana, Turkey

Introduction

The eastern Mediterranean ophiolites in southern Turkey crop out along two belts, namely, Peri-Arabic belt comprising Hatay, Baer Bassit, Troodos, Cilo, Guleman, Zagros and Oman (Ricou 1971), and the Tauride belt along which discontinuous oceanic lithosphere fragments (e.g. Lycian nappes, Ali Hoca complex, Beysehir-Hoyran nappes, Pozanti-Karsanti, Mersin) in association generally with metamorphic sole and ophiolitic melange are seen on both sides of the calcareous axis (Fig. 1a; Juteau 1980; Dilek and Moores 1990). It has been concluded by many authors that most of the ophiolites in Turkey formed in supra-subduction-zone (SSZ) setting (Pearce et al. 1984; Yalınız et al. 1994; Robertson 1994; Parlak et al. 1995b).

Geochemistry of oceanic basalts, mineral chemistry and order of crystallization in ultramafic and mafic cumulates in arc-related/SSZ ophiolite bodies [Troodos (Hébert and Laurent 1990), Bay of Island ophiolite (Elthon et al. 1982; Komor et al. 1985), Border Range ultramafic and mafic complex (Burns 1985; DeBari and Coleman 1989), Klamath mountains (Coleman 1986), California Coast Ranges ophiolites (Shervais 1990)] are inconsistent with traditional low-pressure (1 atm) phase relationships of MORBs.

This paper deals mainly with the whole-rock and mineral chemistry of ultramafic and mafic cumulates and draws attention to high-pressure crystal fractionation features of the Mersin ophiolite magma chamber beneath an island arc/SSZ in southern Turkey within the frame of the Tethyan evolution in the eastern Mediterranean.

Geological frame of the Mersin ophiolite

The Mersin ophiolite complex, one of the discontinuous oceanic lithosphere fragments formed some time during Late Cretaceous in the eastern Mediterranean

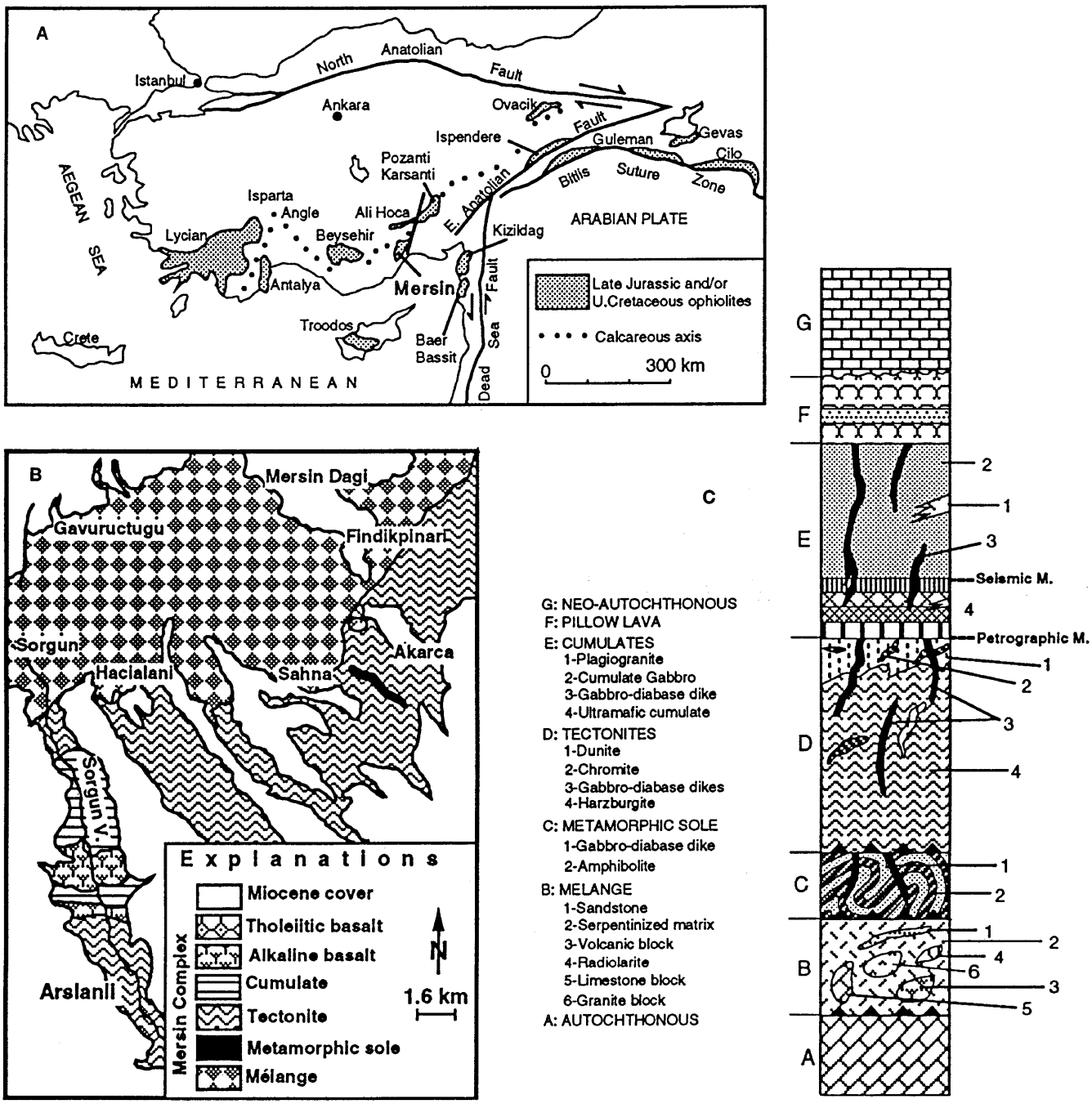

Fig. 1 **A** Ophiolitic massifs in southern Turkey (Modified from Dilek and Moores 1990); **B** simplified geological map of the Mersin ophiolite; **C** Detailed stratigraphic column of the Mersin ophiolite rocks

region, is located in the southern part of the Taurus Calcareous axis in southern Turkey (Fig. 1a; Juteau 1980; Sengor and Yilmaz 1981; Dilek and Moores 1990). This complex having approximately 6 km thickness consists of (in ascending structural order): ophiolitic melange, subophiolitic metamorphics, mantle tectonites, ultramafic and mafic cumulates, alkaline (Late Jurassic–Early Cretaceous)- tholeiitic (Late Cretaceous?) basaltic volcanics in association with deep marine sediments and is tectonically bounded by the Ecemis fault to the east, the Bolkardag metamorphic basement to the north and covered Miocene carbonates to the south and west (Fig. 1).

Well-preserved ultramafic and mafic cumulate rocks are only seen within the roughly N–S oriented Sorgun valley in the western part of the massif (Fig. 1b). The measured detailed stratigraphic section of the cumulates, which was over 3000 m thickness, starts at the bottom with ultrabasic cumulates (800 m) and pass up into gabbroic rocks (2500 m). Basal ultramafic cumulates mainly characterized by adcumulate texture start

with dunites in which stratiform chromites are seen in different levels. Dunites are gradually followed by well-layered wehrlites which in turn are also gradually overlain by clinopyroxenites.The mafic cumulates with mesocumulate, orthocumulate texture start at the bottom with olivine gabbro and continue into gabbro, leucogabbro and anorthosite. In the upper part of the gabbroic cumulates, poorly developed late-stage magma-chamber differentiation products cut also country rock as plagiogranitic inclusions. Igneous lamination, monomineralic size grading and rhythmic layering have been observed as gravity-controlled accumulation structures in the ultramafic and mafic cumulates (Parlak et al. 1995a). Numerous micro-gabbroic-diabasic dikes intrude both types of cumulative rocks. The cumulate has tectonic contact with the tectonites at its base and with basaltic rocks at the top. They show variable attitude of the layering such as E-W/60S, N65E/50NW and N70 W/33NE.

Petrographic summary

The cumulates of the Mersin ophiolite can be subdivided into two groups, namely, ultramafic and mafic cumulates. For the classification and nomenclature of the rocks, Streckeisen (1976) definitions have been followed. Ultramafic cumulates are represented by dunite, wehrlite and clinopyroxenite. Rock units of the ultramafic cumulates preserved their primary textures and they show adcumulate and mesocumulate textures. Pore/trapped liquid component (as a post-cumulus phase) between cumulus minerals in the rock units of the ultramafic cumulates are very limited.The dunites consist of cumulus euhedral olivine 90–95 vol.% ($Fo_{90–85}$) with grain size of 1.5–3 mm and 1–5 vol.% chromian spinel (Cr# 60–80%) with the grain size between 0.7–1 mm. The wehrlites are represented by 25–35 vol.% olivine and euhedral–subhedral (55–75 vol.%) clinopyroxene with the grain size of 0.5–5 mm. The composition of the clinopyroxene ranges from (En_{s45} Fs_4 Wo_{47}) to (En_{s48} Fs_9 Wo_{49}). The clinopyroxenite contains adcumulus coarse grained euhedral (1–8.5 mm) clinopyroxenes.

The mafic cumulates consisting mainly of gabbro, leucogabbro, olivine gabbro and anorthosite constitute almost two thirds of whole cumulate section. The mafic cumulative rocks are very fresh and they present adcumulate, mesocumulate and orthocumulate texture. The gabbros consist mainly of 50–55 vol.% calcic plagioclase ($An_{95–91}$) with the grain size between 1–3 mm, 35–45 vol.% clinopyroxene ($En_{40–45}$ $Fs_{8–12}$ $Wo_{46–47}$) with 0.5–2 mm grain size and intercumulus anhedral 2–5 vol.% orthopyroxene with grain size of 0.5–0.8 mm. The gabbro with olivine contains cumulus 20–25 vol.% olivine ($Fo_{80–81}$) with grain size of 0.8–2.5 mm, 55–60 vol.% plagioclase and 15–20 vol.% clinopyroxene. The leucogabbros are made of 65–70 vol.% cumulus plagioclase and 30–35 vol.% clinopyroxene. The anorthosite contains adcumulate (99 vol.%) euhedral highly calcic plagioclase ($An_{91.6–95.6}$) with the grain size between 2 and 5.2 mm and 1 vol.% clinopyroxene filling the interstices of the cumulus plagioclases as post-cumulus mineral.

Analytical technique

A total of 21 samples from ultramafic and mafic cumulates have been analysed in terms of major and trace element concentrations. Major and trace element analyses have been carried out by XRF in the Mineralogy Department at the University of Geneva. Major and trace element compositions were determined on glass beads fused from ignited powders to which $Li_2B_4O_7$ was added (1:5), in a gold-platinum crucible at 1150°C. A total of 30 representative thin sections were used for micro probe analysis on a Camebax SX-50 in the Mineralogy Department at Lausanne University. The analytical conditions for the elements [(K = Orthose), (Si = Diopside, Olivine, Albite), (Mg = Diopside, Olivine), (Ca = Wollastonite, Anorthite), (Al = Jadeite, Anorthite), (Na = Jadeite, Albite), (Mn = Mns1, $MnTiO_3$), (Cr = Cr_2O_3), (Ti:Ilmenite, $MnTiO_3$), (Fe = Hedenbergite, Fe_2O_3), (Ni = NiO)] were 20 s of counting interval, beam current –20 mA and acceleration voltage –15 kV.

Whole-rock chemistry

The cumulative rocks in the Mersin ophiolite range from highly magnesian (40–17 wt.%) in dunites, wehrlites and clinopyroxenite to less magnesian (5–10 wt.%) in more evolved rocks such as gabbro, gabbro with olivine and anorthosite characterized by high CaO (15–18 wt.%) and Al_2O_3 (34–18 wt.%) contents (Table 1). The overall trend from Mg-rich to Ca- and Al-rich cumulates is directly associated with the formation of the layered sequences by magmatic accumulation of olivines, clinopyroxenes and plagioclases in the Mersin ophiolite magma chamber. Major element compositions of the ultramafic and mafic cumulates are plotted in the AFM diagram (Beard 1986): The dunites and wehrlites show Mg enrichment, whereas gabbros are on the arc-cumulate gabbro field (Fig. 2); however, two samples from the ultramafic cumulates plot on the arc-cumulate gabbro field. Trace element abundances vary with both modal mineralogy (including amount of post-cumulus mineral) and Mg number of rock units (Jaques et al. 1983). Trace element concentrations in the ultramafic and mafic cumulates of the Mersin ophiolite are well correlated with the fractionation of olivine, chrom-spinel, pyroxene and Ca-plagioclase. Cr and Ni contents are high in the dunites and wehrlites (1900–200 ppm Ni, 7500–1500 ppm Cr; Fig. 3) and decrease lower values in gabbroic rocks (Ni <60 ppm , Cr <250 ppm). Sr concentrations increase with the modal

Table 1 Whole rock (major and trace) chemical analyses of ultramafic and mafic cumulates

Rock	Whr	D	Whr	Whr	D	D	Whr	Cpxt	Cpxt	G+olv	Whr	Whr	G	Whr	G	G	G	G+olv	Whr	Whr	Anrt
No.	11	12	13	14	15	16	17	19	20	21	22	23	24	25	28	31	35	36	37	46	325
SiO_2	51.40	35.34	51.39	48.1	35.05	34.47	51.57	50.62	52.82	47.2	49.68	49.04	46.88	41.91	47.6	47.75	47.92	43.88	41.58	52.59	45.15
TiO_2	0.05	0.01	0.05	0.05	0.02	0.02	0.07	0.09	0.08	0.06	0.09	0.05	0.08	0.05	0.07	0.06	0.05	0.02	0.08	0.06	0.03
Al_2O_3	1.15	0.27	1.15	1.06	0.23	0.28	1.85	2.52	2.46	17.37	2.28	1.29	18.14	15.7	22.21	21.6	19.95	27.6	3.51	1.37	33.77
FeO*	4.20	8.67	4.44	5.09	9.48	7.75	4.93	5.13	4.29	4.10	5.04	5.46	6.55	6.92	6.23	3.54	5.48	2.56	12.54	4.43	0.72
MgO	23.28	40.54	23.78	25.50	40.72	42.31	21.28	19.83	18.45	11.39	19.1	23.97	10.58	16.66	7.57	7.72	10.19	5.68	27.25	20.19	0.23
MnO	0.10	0.14	0.11	0.10	0.14	0.11	0.11	0.11	0.10	0.08	0.1	0.11	0.12	0.1	0.11	0.07	0.12	0.04	0.19	0.1	0.01
CaO	18.31	1.60	17.97	14.60	1.13	0.51	19.20	19.38	20.93	18.38	18.66	16.05	14.57	12.8	15.63	17.53	15.25	17.37	8.17	20.38	18.08
Na_2O	0.01	0.05	<	<	0.17	0.12	<	<	0.12	0.30	0.16	<	0.55	0.13	0.55	0.44	0.37	0.52	<	0.24	1.09
K_2O	<	<	<	<	0.01	0.01	<	<	<	<	<	<	<	<	<	<	<	<	0.04	<	0.01
P_2O_5	0.01	0.01	0.01	0.01	0.01	<	0.01	0.01	0.01	0.01	0.01	0.01	0.01	0.01	0.01	0.01	0.01	0.01	0.01	0.01	0.01
LOI	1.18	13.71	0.76	5.16	13.00	14.68	1.05	2.20	0.81	1.29	4.82	3.32	2.30	5.38	0.51	1.45	0.58	1.91	5.92	0.57	1.07
Total	99.33	100.40	99.66	99.67	99.96	100.30	100.10	99.89	100.10	100.20	99.95	99.3	99.78	99.66	100.30	100.20	99.92	99.59	99.29	99.94	100.10
ppm																					
Ba	<	<	18	<	<	<	<	31	3	<	<	<	<	16	<	3	<	<	39	16	<
Ni	342	1136	367	499	1578	1915	283	192	176	113	385	388	55	416	56	63	36	109	583	239	38
Cr	3658	7480	3963	3446	5542	6698	2456	1663	1665	259	2173	1429	152	1491	92	244	29	140	1307	3213	17
V	98	38	89	85	31	44	153	183	169	115	163	123	151	83	111	98	117	43	146	110	20
Nb	1	1	1	1	5	<	5	0	3	1	1	4	1	<	1	1	1	1	<	3	4
Zr	8	7	4	7	6	6	5	6	8	8	7	6	9	8	11	10	10	13	6	9	13
Y	14	11	13	14	11	4	14	13	5	14	13	14	14	12	14	14	14	14	12	10	<
Rb	5	5	1	1	1	6	4	2	1	<	1	<	5	1	2	1	2	<	<	9	6
Sr	<	<	<	<	<	3	<	0	<	51	<	3	59	42	81	87	69	98	<	<	179

NOTE: FeO* is expressed as total Fe, < means below detection limit

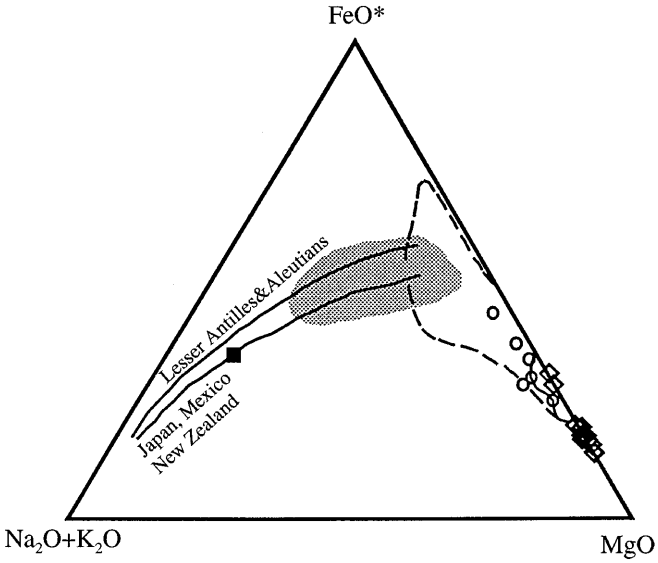

Fig. 2 AFM composition of ultramafic (*open diamond*) and mafic cumulates [(gabbro (*open circles*) and anorthosite (*filled diamond*)] in the Mersin ophiolite. *Dashed line* indicates arc-related mafic cumulate field. *Solid line* represents field of arc-related ultramafic cumulates. *Shaded area* indicates arc-related non-cumulate gabbro and diorite. Fields of cumulate and non-cumulate rocks are from Beard (1986), and arc volcanic trends are from Brown (1982)

abundance of plagioclase (40–90 ppm) in the gabbros and reach as high as 179 ppm in the anorthosite. Incompatible trace elements (Zr, Ba, Rb, Nb, Y etc.) generally show moderate to low concentrations (Table 1), which may be deduced from the high-cumulus-phase activity in the magma chamber of the Mersin ophiolite.

Mineral chemistry

Olivine

Olivine compositions in the ultramafic–mafic cumulates and mantle tectonites present variations depending mainly on lithology (Table 2). Olivine crystals do not show compositional zoning from core to rim and are generally uniform in composition within individual samples. Olivine is highly magnesian in harzburgite tectonites ($Fo_{91.5–90}$), basal dunites–wehrlites ($Fo_{89.5–86}$) and decreases gradually in olivine gabbro ($Fo_{81.5–80}$) with a small degree of differentiation in the magma chamber. Similarity of olivine compositions in the lowest cumulates and underlying mantle peridotite suggest that the parental magma for the cumulates equilibrated with mantle-type olivine (Pallister and Hopson 1981). The NiO content is positively correlated with Mg# and higher in harzburgite (0.43–0.36 wt.%) compared with the ultramafic cumulates (0.25–0.12 wt.%; Table 2). The Cr_2O_3 content in olivines is negligible (<0.1 wt.%) both in basal cumulates and olivine gabbros.

In cumulates olivine is the first crystallizing cumulus mineral phase coexisting together with chromian spinels in dunites. Olivines are also present in plagioclase-rich rocks and relatively less magnesian ($Fo_{81.5–80}$) rich. This high Mg nature of olivines in the ultramafic and mafic cumulates of the Mersin ophiolite differ from differentiated oceanic equivalents (Hébert 1982, 1985; Elthon 1987). The olivine compositions in the cumulative rocks of the Mersin ophiolite show close similarities to those such as Troodos ophiolite (Hébert and Laurent 1990), Tossina complex (DeBari and Coleman 1989), Border Range ultramafic and mafic complex (Burns 1985) and Bay of Island ophiolite (Elthon et al. 1982), which are thought to have formed in an arc environment.

Chromian spinel

The spinel compositions in the basal ultramafic cumulates and in the mantle tectonites of the Mersin ophiolite are rich in Cr_2O_3 (61–49 wt.%), low in Al_2O_3 (19–9 wt.%) and the Cr# (100*Cr/Cr+Al) ranges from 60 to 80 (Table 3). The chromian spinel compositions in the Mersin ophiolite are different from those of oceanic crust (Dick and Bullen 1984) and stratiform complexes (Irvine 1967) and similar to chromian spinels from Troodos ophiolite (Hébert and Laurent 1990) and Border Ranges ultramafic and mafic complex (Burns 1985). Dick and Bullen (1984) suggested that spinels with high Cr# (>60%) are restricted to volcanic arcs, stratiform complexes and oceanic plateau basalts, whereas low Cr# (<60%) in spinels is typical of oceanic crust. Thus, on the basis of above-mentioned interpretations the compositions of chromian spinels in the Mersin ophiolite suggest arc-related tectonic environment (Fig. 4).

Clinopyroxene

Representative clinopyroxene compositions from ultramafic and mafic cumulates of the Mersin ophiolite are given in Table 4. The clinopyroxenes from ultramafic cumulates demonstrate very restricted compositional variations (En_{49-45} $Wo_{50–45}$ $Fs_{6–3}$) and are in the diopside field (Fig. 5). The clinopyroxenes from gabbroic cumulates show weak Fe enrichment ($En_{49–45}$ $Wo_{48–45}$ $Fs_{10–7}$) with differentiation and plot in the diopsite field (Fig. 5).

The most conspicuous feature of the clinopyroxenes in the ultramafic and mafic cumulates is the extremly high Mg number (95–85 and 85–77, respectively). The Cr_2O_3 in clinopyroxene is plotted against the Mg number in Fig. 6a. Cr_2O_3 content in the clinopyroxenes of the basal cumulate is higher and is decreasing with decreasing Mg# in the gabbroic clinopyroxenes (Fig. 6a). This feature could be related to the gradual Cr impoverishment of the magma (Hodges and Papike 1976). A

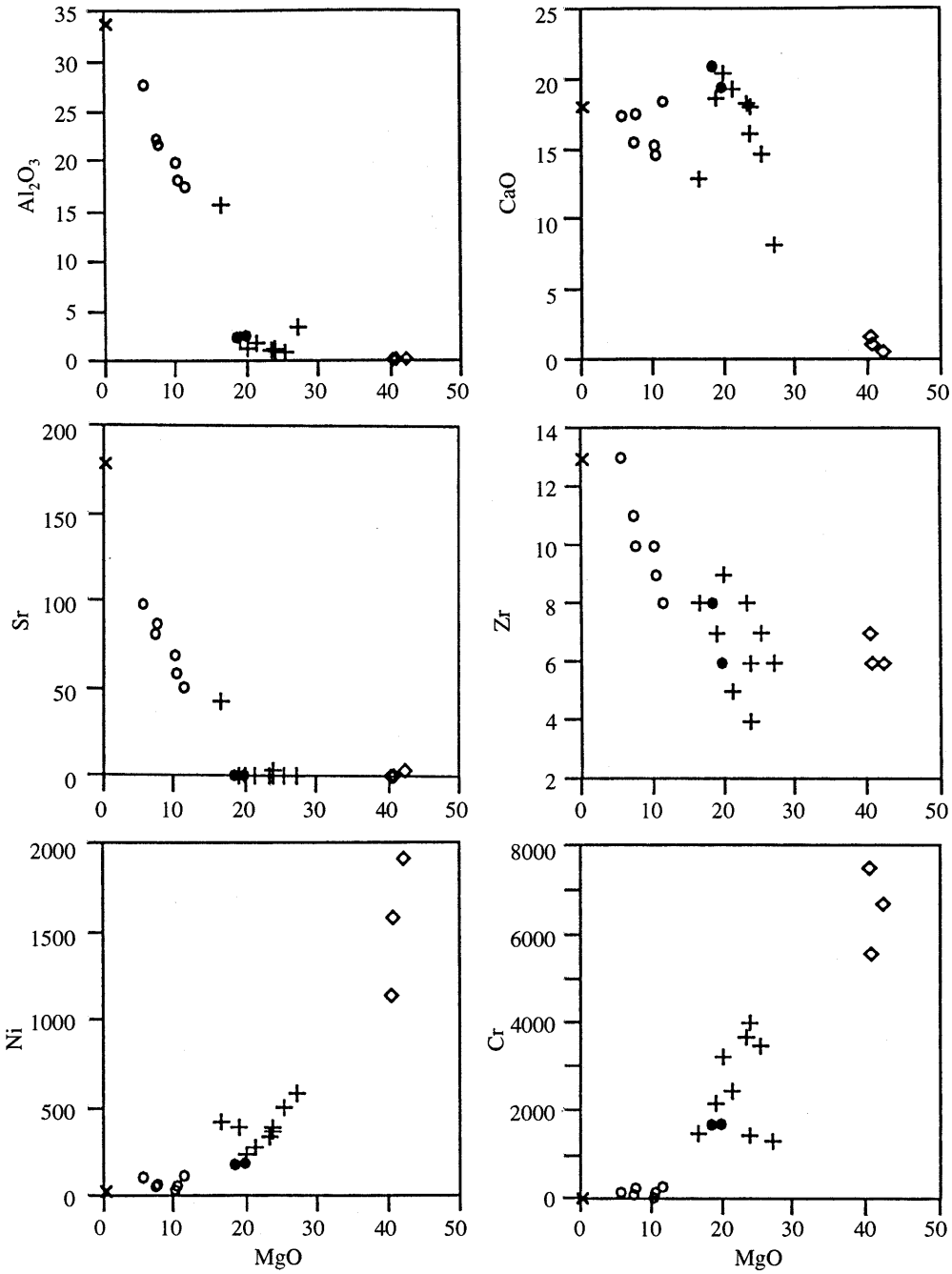

Fig. 3 Selected major and trace element variations of the ultramafic [dunite (*diamond*), wherlite (*crosses*), clinopyroxenite (*filled circles*)] and mafic cumulates [gabbro (*open circles*), anorthosite (×)] with MgO as a differentiation index in the Mersin ophiolite. Ni and Cr are positively correlated, whereas Sr, Zr, Al_2O_3 and CaO are negatively correlated with MgO, indicating progressive differentiation in the magma chamber

similar relationship is observed in the ultramafic and gabbroic cumulates of Troodos (Hébert and Laurent 1990) and North Arm Mountain massif of the Bay of Island ophiolite complex (Elthon et al. 1982, 1984; Komor et al. 1986).

Magnesium number vs TiO_2 in the clinopyroxenes of the ultramafic and gabbroic cumulates from the Mersin ophiolite is shown in Fig. 6b. Elthon (1987) declared that the clinopyroxenes with high Mg numbers also have high TiO_2. This general feature does not fit with the Mersin ophiolite case, because the clinopyroxenes with higher Mg number have generally lower TiO_2 (<0.1 wt.%) (Fig. 6b). The Mersin relation is seen in Bay of Island ophiolite complex (Elthon et al. 1982, 1984; Komor et al. 1985) and in Troodos ophiolite (Hébert and Laurent 1990). TiO_2 content of clinopyroxene generally depends on cooling rate, with faster cooling rates increasing the apparent distribution of Ti coefficient (Coish and Taylor 1979; Gamble and Taylor 1980; Elthon 1987). Consequently, TiO_2 content of clinopyroxenes in the volcanic rocks of the Mersin ophiolite have higher TiO_2 (0.96–0.5 wt.%) compared with the cumulative rocks (Fig. 6b). Ti content of clinopyroxene reflects the degree of depletion of mantle source and the Ti activity of parent magma which generated cumulate suite (Pearce and Norry 1979). The magma source from which the clinopyroxenes crystallized was poor in Ti in the Mersin ophiolite. Absence of zoning and con-

Table 2 Representative olivine analyses from ultramafic cumulates and mantle tectonites

	Mantle tectonite			Ultramafic cumulate															
	Harzburgite			Wehrlite												Dunite			
Sample no.	68-2c	68-3c	68-4c	11-1c	13-7c	14-4c	17-3c	22-4c	23-5c	46-1c	46-2c	46-3c	46-4c	46-5c	46-6c	15-2c	30-1c	30-2c	30-3c
SiO_2	40.75	40.82	40.99	41.01	40.55	41.29	40.55	40.22	40.91	40.16	40.17	40.12	40.10	39.78	40.24	40.97	40.81	40.43	40.72
TiO_2	<	<	<	<	0.03	<	0.01	<	<	0.01	<	0.02	<	0.02	<	<	0.01	0.01	0.02
Al_2O_3	<	<	0.01	0.02	<	<	0.01	0.01	0.01	<	<	<	<	<	<	<	<	0.02	<
FeO*	8.44	8.31	8.30	10.81	10.93	10.09	13.22	13.97	11.81	12.87	12.79	13.15	13.01	13.03	12.89	10.57	10.54	10.75	10.76
Cr_2O_3	0.01	<	0.01	0.03	0.05	0.05	0.02	<	<	0.03	<	<	0.00	0.01	<	0.06	<	0.03	0.01
MnO	0.10	0.14	0.07	0.15	0.19	0.13	0.29	0.21	0.22	0.12	0.16	0.20	0.22	0.16	0.14	0.18	0.15	0.18	0.17
MgO	50.24	50.44	50.59	47.73	46.86	47.83	45.81	44.79	47.06	46.80	47.02	47.23	47.12	46.88	46.94	48.05	48.74	48.74	48.51
CaO	0.01	<	0.01	0.01	0.03	0.03	<	<	0.04	0.01	0.01	0.05	0.02	0.03	0.02	0.01	0.03	0.02	0.04
Na_2O	<	<	<	<	<	<	0.03	0.01	<	<	<	<	<	<	<	<	<	<	<
K_2O	<	<	<	0.02	<	<	<	<	0.01	<	<	<	<	<	<	0.01	<	<	<
NiO	0.39	0.36	0.43	n.d.	n.d.	n.d.	n.d.	n.d.	n.d.	0.15	0.18	0.12	0.14	0.12	0.15	n.d.	0.25	0.19	0.15
Total	99.94	100.08	100.41	99.78	98.64	99.42	99.94	99.21	100.06	100.15	100.33	100.89	100.61	100.03	100.40	99.85	100.53	100.37	100.38
Si	0.99	0.99	1.00	1.01	0.98	1.00	1.01	0.99	1.01	1.00	1.00	0.99	0.99	0.99	1.00	1.00	1.00	0.99	1.00
Ti	<	<	<	<	0.00	<	0.00	<	<	0.00	<	0.001	<	0.00	<	<	0.00	0.00	0.00
Al	<	<	0.00	0.00	<	<	0.00	0.00	0.00	<	<	<	<	<	<	<	<	0.00	<
Fe	0.17	0.17	0.17	0.22	0.22	0.21	0.27	0.29	0.24	0.27	0.27	0.27	0.27	0.27	0.27	0.22	0.22	0.22	0.22
Cr	0.00	<	0.00	0.00	0.00	0.00	0.00	<	<	0.00	<	<	0.00	0.00	<	0.00	<	0.00	0.00
Mn	0.00	0.00	0.00	0.00	0.00	0.00	0.01	0.00	0.00	0.00	0.00	0.00	0.00	0.00	0.00	0.00	0.00	0.00	0.00
Mg	1.83	1.83	1.83	1.74	1.69	1.73	1.70	1.65	1.73	1.73	1.74	1.74	1.74	1.74	1.73	1.76	1.78	1.78	1.77
Ca	0.00	<	0.00	0.00	0.00	0.00	<	<	0.00	0.00	0.00	0.00	0.00	0.00	0.00	0.00	0.00	0.00	0.00
Na	<	<	<	<	<	<	0.00	0.00	<	<	<	<	<	<	<	<	<	<	<
K	<	<	<	0.00	<	<	<	<	0.00	<	<	<	<	<	<	0.00	<	<	<
Ni	0.01	0.01	0.01	n.d.	n.d.	n.d.	n.d.	n.d.	n.d.	0.00	0.00	0.00	0.00	0.00	0.00	n.d.	0.01	0.00	0.00
Fo (100*Mg/Mg+Fe)	91.31	91.41	91.51	88.73	88.43	89.42	86.07	85.11	87.66	86.53	86.62	86.36	86.41	86.39	86.53	89.02	89.09	88.85	88.83
Fa (100*Fe/Fe+Mg)	8.61	8.45	8.43	11.27	11.57	10.58	13.93	14.89	12.34	13.35	13.22	13.50	13.39	13.48	13.35	10.98	10.81	11.00	11.05
Mg*(100*Mg/Mg+Fe)	91.50	91.50	91.50	88.59	88.25	89.30	85.80	84.92	87.46	86.50	86.60	87.00	86.60	86.60	86.50	88.85	89.00	89.00	88.90

NOTE: Number of ions on the basis of 4 (O); total Fe is expressed as FeO*; n.d. not determined; < means below detection limit

Table 3 Representative chromian-spinel analyses from mantle tectonites and ultramafic cumulates

	Ultramafic cumulate			Mantle tectonite	
	Dunite			Harzburgite	
No.	5-1cr	12-1cr	15-1cr	73-1	90-1
SiO_2	0.05	0.12	0.08	0.04	0.07
TiO_2	0.15	0.21	0.24	0.02	<
Al_2O_3	8.90	10.27	10.30	15.10	18.90
Cr_2O_3	60.33	55.60	52.09	53.45	49.93
FeO*	18.99	25.30	28.41	20.14	19.11
MnO	0.34	0.44	0.44	0.29	0.21
MgO	10.69	7.79	7.68	10.25	11.00
CaO	<	0.02	0.01	<	0.02
Na_2O	<	0.01	0.01	<	0.03
K_2O	0.01	<	<	<	<
Total	99.46	99.76	99.26	99.29	99.27
Si	0.01	0.03	0.02	0.01	0.02
Ti	0.03	0.04	0.05	0.00	<
Al	2.76	3.26	3.28	4.56	5.58
Cr	12.56	11.85	11.12	10.82	9.88
Fe	4.18	5.71	6.41	4.31	4.00
Mn	0.08	0.10	0.10	0.06	0.04
Mg	4.20	3.13	3.09	3.91	4.11
Ca	<	0.01	0.00	<	0.01
Na	<	0.01	0.01	<	0.01
K	0.00	<	<	<	<
Cr # (100*Cr/Cr + Al)	81.97	78.41	77.23	70.37	63.93
Fm # (100*Fe/Mg + Fe)	49.91	64.56	67.48	52.43	49.35

NOTE: Number of ions on the basis of 32 (O); total Fe is expressed as FeO; < means below detection limit

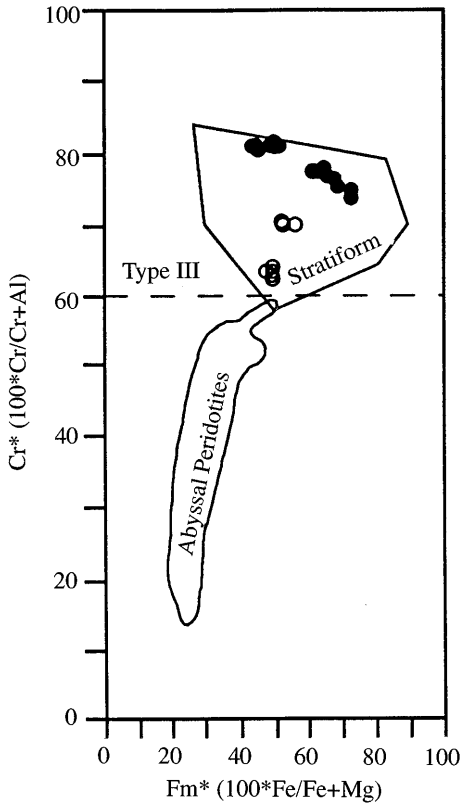

Fig. 4 Spinel compositions from ultramafic cumulates (*filled circles*) and peridotites (*open circles*) in the Mersin ophiolite. Type-III spinel field and abyssal peridotite field from Dick and Bullen (1984), and stratiform field from Irvine (1967)

sistent compositions in the cumulus and intercumulus phases indicate slow cooling and extensive subsolidus re-equilibration (Burns 1985). These features support also crystallization at high pressures in the oceanic crust.

The Al_2O_3 content of the clinopyroxene against Mg number for ultramafic and gabbroic cumulates is plotted in Fig. 6c. The clinopyroxenes from ultramafic cumulates show a low amount of Al_2O_3 (<4 wt.%) and are approximately perpendicular to the trend of Skaergaard and Semail ophiolite which are thought to be low-pressure crystallization products. The trend of clinopyroxenes is compatible with the trend of high-pressure peridotites from southwestern Oregons (Medaris 1972) as well as the trend of Aleutian lower crustal units (DeBari et al. 1987; Conrad and Kay 1984), whereas the clinopyroxenes from gabbroic rocks follow Skaergaard and Semail trend (Fig. 6c). Furthermore, Al (VI) vs Al (IV) plot of clinopyroxenes, which permits to define high-low pressure crystallization (Aoki and Kushiro 1968), are in the field of granulites and high-pressure xenoliths (Fig. 6d).

Orthopyroxene

Orthopyroxenes are absent in the ultramafic cumulates and rarely observed in the high-level gabbroic cumulates as intercumulus phase (Table 5). They are hypersthene in composition (Fig. 5). The Mg number ($Mg\#_{68-77}$) of orthopyroxenes is lower and they are Fe-enriched. Cr_2O_3 content of orthopyroxenes are negligible again suggesting Cr decrease in the basaltic li-

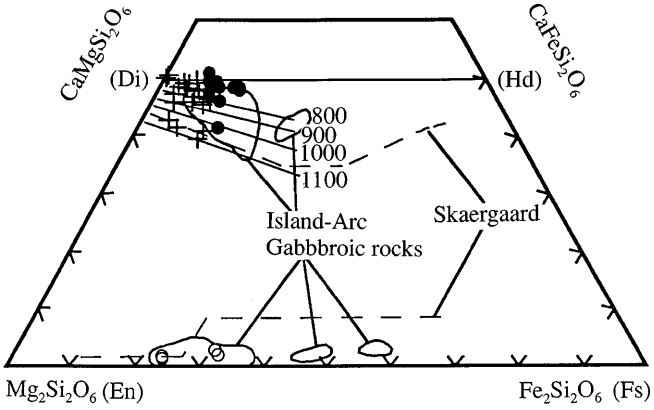

Fig. 5 Pyroxene ternary diagram showing clinopyroxene and orthopyroxene compositions from ultramafic and mafic cumulates. *Crosses* indicate clinopyroxene from ultramafic and *filled circles* indicate clinopyroxene from gabbroic cumulates. *Open circles* are Opx in the gabbroic cumulates. Temperature estimates in degrees Celsius from Ross and Huebner (1975). Fields of island-arc gabbroic rocks (*solid lines*) and Skaergaard trend are from Burns (1985)

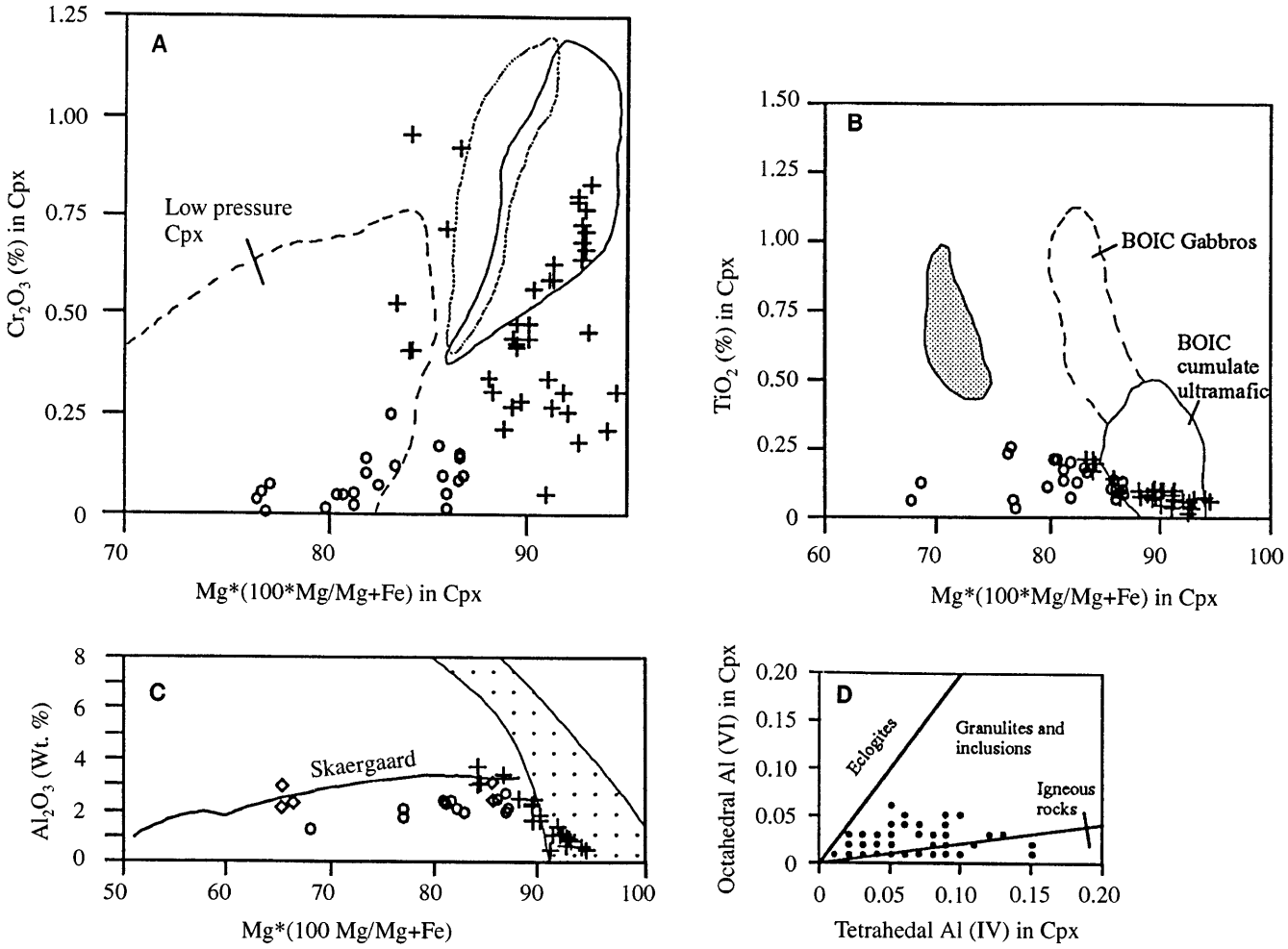

Fig. 6 **A** Cr_2O_3 vs Mg number in clinopyroxene in the ultramafic (*crosses*) and mafic (*open circles*) cumulates. Low-pressure Cpx field from 1-atm experimental studies of N-MORB (Elthon 1987). Bay of Island ultramafic (*solid line*) and mafic (*dashed line*) cumulates are also shown (after Elthon 1987). **B** TiO_2 vs Mg number (100*Mg/Mg+Fe) in clinopyroxenes from ultramafic (*crosses*) and mafic (*open circles*) cumulates. *Shaded area* is the volcanic clinopyroxene compositions in the Mersin ophiolite. *Dashed* and *solid line* indicate gabbro and ultramafic cumulate field of the Bay of Island ophiolite, respectively (after Elthon 1987). **C** Trend of moderate increasing of Al_2O_3 vs decreasing Mg# in clinopyroxenes of the ultramafic and mafic cumulates of the Mersin ophiolite. Field of high-pressure peridotite (*dotted area*) after Medaris (1972). Trend of gabbroic cumulates (*open circles*) parallel to the trend of low-pressure cumulates such as Skaergaard intrusion and Semail ophiolite (*open diamond*; from DeBari and Coleman 1989). **D** Al in octahedral vs tetrahedral coordination in clinopyroxenes. High octahedral-to-tetrahedral ratios indicate higher pressures of formation. Fields are from Aoki and Kushiro (1968). *Filled circles* indicate ultramafic and mafic cumulates of the Mersin ophiolite, plotting in the field of granulite and high-pressure xenoliths

quid with differentiation. Al_2O_3 content (1.4–1.9 wt.%) is slightly lower than the coexisting clinopyroxenes. The same features have been observed in the Tossina complex and interpreted as low-pressure igneous intrusion (DeBari and Coleman 1989).

Plagioclase

In gabbroic cumulates plagioclase, which is not observed within the ultramafic cumulates, is the major crystallizing phase and highly calcic in the compositional range from An_{96} to An_{90} (Table 6). This very limited compositional range of plagioclase in the gabbroic rocks of the Mersin ophiolite differs from those plagioclases in mid-oceanic ridge gabbros (Burns 1985; Hébert 1982), and similar variations have been observed in the Troodos cumulate sequence (Hébert and Laurent 1990) and arc-related plutonic rocks (DeBari and Coleman 1986, 1989; DeBari et al. 1987; Arculus and Wills 1980; Dupuy et al. 1982; Beard 1986; Fujimaki 1986). The Or content of plagioclases in the gabbros is negligible (less than 0.1 wt.%). Or-poor plagioclases are also reported from the Troodos ophiolite (Hébert and Laurent 1990), the Lesser Antilles (Arculus and Wills 1980) and the Peninsular Ranges Batholiths (Smith et al. 1983).

Origin of calcic plagioclase has been outlined in the literature in following ways such as experimental work carried out on the Albite–Anorthite water system (Johannes 1978) showed that high water pressure could cause plagioclase compositions to be anorthite rich.

Table 4 Representative clinopyroxene analyses from ultramafic and mafic cumulates

	Ultramafic cumulates								Mafic cumulates					
	Wehrlite								Cpxt	Cpxt	Gol + ol_r	Gabbro		
No.	11-1c	13-1c	14-1c	17-1c	18-1c	22-1c	23-1c	25-1c	19-1c	20-1c	21-1c	24-1c	28-1c	31-1c
SiO_2	54.47	54.14	55.10	53.65	53.06	53.11	54.48	51.87	53.07	54.46	52.53	52.17	53.01	52.67
Al_2O_3	1.09	1.06	0.61	1.76	1.95	2.41	0.76	3.55	2.54	0.61	2.81	2.49	1.40	2.22
TiO_2	0.06	0.03	0.06	0.10	0.05	0.10	0.04	0.08	0.08	0.04	0.10	0.22	0.07	0.21
FeO*	2.27	2.33	1.78	3.25	3.59	3.52	2.41	4.31	3.45	2.94	4.44	6.64	20.02	6.29
MnO	0.15	0.12	0.12	0.08	0.12	0.10	0.15	0.21	0.07	0.15	0.11	0.20	0.33	0.21
MgO	17.24	17.11	17.26	16.49	16.66	16.56	17.13	15.32	16.18	16.72	15.74	15.09	23.72	15.79
Cr_2O_3	0.69	0.71	0.31	0.48	0.44	0.43	0.18	0.92	0.28	0.05	0.08	0.04	0.04	0.10
CaO	24.41	24.11	25.29	24.12	23.81	24.27	25.10	23.82	23.84	24.99	23.57	23.01	1.01	22.44
Na_2O	0.11	0.10	0.04	0.08	0.16	0.11	0.02	0.20	0.10	0.00	0.13	0.20	<	0.18
K_2O	0.02	0.02	<	0.01	0.82	<	0.01	0.01	<	<	0.03	0.14	<	0.09
Total	100.51	99.73	100.57	100.02	100.66	100.61	100.28	100.29	99.61	99.96	99.54	100.20	99.60	100.20
Si	1.97	1.94	1.99	1.96	1.93	1.93	1.98	1.90	1.90	1.98	1.88	1.92	1.91	1.93
Al IV	0.03	0.04	0.01	0.04	0.07	0.07	0.02	0.10	0.10	0.02	0.12	0.08	0.06	0.07
Al VI	0.02	0.00	0.01	0.03	0.01	0.03	0.01	0.05	0.01	0.01	0.00	0.03	0.00	0.03
Ti	0.00	0.00	0.00	0.00	0.00	0.00	0.00	0.00	0.00	0.00	0.00	0.01	0.00	0.01
Fe	0.07	0.07	0.05	0.10	0.10	0.11	0.07	0.13	0.10	0.09	0.13	0.20	0.06	0.19
Mn	0.00	0.00	0.00	0.00	0.00	0.00	0.00	0.01	0.00	0.00	0.00	0.01	0.01	0.01
Mg	0.93	0.92	0.93	0.90	0.90	0.90	0.93	0.84	0.86	0.91	0.84	0.83	1.28	0.86
Cr	0.02	0.02	0.01	0.01	0.01	0.01	0.01	0.03	0.01	0.00	0.00	0.00	0.00	0.00
Ca	0.95	0.93	0.98	0.94	0.93	0.94	0.98	0.93	0.91	0.97	0.90	0.91	0.04	0.88
Na	0.01	0.01	0.00	0.01	0.01	0.01	0.00	0.01	0.01	0.00	0.01	0.01	<	0.01
K	0.00	0.00	<	0.00	0.04	<	0.00	0.00	<	<	0.00	0.01	<	0.00
En (100*Mg/(Mg + Fe + Ca)	47.70	47.78	47.29	46.20	49.23	45.96	46.80	43.80	45.85	45.92	44.68	43.93	66.14	45.33
Fs (100*Fe/(Mg + Fe + Ca)	3.76	3.84	2.92	5.23	0.20	5.64	3.93	7.25	5.60	4.76	7.25	7.92	31.83	8.34
Wo (100*Ca/(Mg + Fe + Ca)	48.54	48.38	49.79	48.56	50.27	48.40	49.28	48.94	48.55	49.32	48.08	48.15	2.02	46.32
Mg* (100*Mg/(Mg + Fe)	92.61	92.90	94.88	89.98	90.00	89.06	92.98	86.53	89.62	90.98	86.59	80.58	95.51	81.90
Cr# (Cr/Cr + Fe)	0.21	0.22	0.15	0.12	0.09	0.10	0.07	0.17	0.07	0.02	0.02	0.00	0.02	0.00

NOTE: Number of ions on the basis of 6 (O); total Fe is expressed as FeO*; < means below detection limit

Table 5 Representative Orthopyroxene analyses from mafic cumulates

	Mafic cumulates					
	Leuco-gabbro					
No.	28-1c	28-3c	35-1c	35-4c	35-7c	35-8c
SiO_2	53.01	53.05	54.43	54.55	54.53	54.48
Al_2O_3	1.40	1.62	1.86	1.93	1.63	1.59
TiO_2	0.07	0.13	0.07	0.04	0.05	0.08
FeO*	20.02	19.31	14.93	14.54	15.20	14.72
MnO	0.33	0.43	0.45	0.36	0.32	0.38
MgO	23.72	23.65	27.74	27.37	27.83	27.29
Cr_2O_3	0.04	<	<	0.07	<	<
CaO	1.01	1.28	0.80	0.84	0.74	0.82
Na_2O	<	0.02	0.03	<	0.02	<
K_2O	<	0.01	<	0.02	0.01	<
Total	99.60	99.50	100.31	99.72	100.33	99.36
Si	1.91	1.90	1.95	1.93	1.95	1.90
Al IV	0.06	0.07	0.05	0.07	0.05	0.07
Al VI	0.00	0.00	0.03	0.01	0.02	0.00
Ti	0.00	0.00	0.00	0.00	0.00	0.00
Fe	0.60	0.58	0.45	0.43	0.45	0.43
Mn	0.01	0.01	0.01	0.01	0.01	0.01
Mg	1.28	1.26	1.48	1.44	1.48	1.42
Cr	0.00	<	<	0.00	<	<
Ca	0.04	0.05	0.03	0.03	0.03	0.03
Na	<	0.00	0.00	<	0.00	<
K	<	0.00	<	0.00	0.00	<
En (100*Mg/Mg + Fe + Ca)	66.14	66.35	75.09	75.33	75.08	75.07
Fs (100*Fe/Mg + Fe + Ca)	31.83	31.07	23.36	23.01	23.49	23.31
Wo (100*Ca/Mg + Fe + Ca)	2.02	2.58	1.56	1.66	1.43	1.62
Mg# (100*Mg/Mg + Fe)	68.03	68.56	76.68	77.05	76.74	76.72

NOTE: Number of ions on the basis of 6 (O); total Fe is expressed as FeO*; < means below detection limit

Table 6 Representative plagioclase analyses from gabbroic cumulates

	Mafic cumulates						
	G + ol_r		Gabbro		Leuco-gabbro		Anorthosite
No.	21-10c	36-5c	24-4c	31-6c	28-2c	35-3c	325-6c
SiO_2	43.93	44.30	44.38	44.47	45.02	43.74	44.83
Al_2O_3	35.53	35.15	35.60	35.13	34.45	35.54	34.41
TiO_2	<	0.01	<	<	0.02	0.02	0.02
FeO*	0.16	0.23	0.25	0.21	1.09	0.24	0.44
MnO	<	<	<	<	0.02	0.02	0.05
MgO	<	<	<	<	0.05	0.01	0.04
CaO	20.00	19.66	19.03	18.74	18.64	19.41	18.85
Na_2O	0.46	0.61	0.71	0.89	1.08	0.57	0.87
K_2O	<	<	0.01	<	0.02	<	<
Total	100.08	99.96	99.98	99.45	100.39	99.55	99.61
Si	2.03	2.05	2.05	2.07	2.07	2.03	2.08
Al IV	0.97	0.95	1.94	1.92	0.93	0.97	0.92
Al VI	0.96	0.96			0.94	0.97	0.96
Ti	<	0.00	<	<	0.00	0.00	0.00
Fe	0.01	0.01	0.01	0.01	0.04	0.01	0.02
Mn	<	<	<	<	0.00	0.00	0.00
Mg	<	<	<	<	0.00	0.00	0.00
Ca	0.99	0.97	0.94	0.93	0.92	0.96	0.94
Na	0.04	0.05	0.06	0.08	0.10	0.05	0.08
K	<	<	0.00	<	0.00	<	<
Ab (100*Na/(K + Ca + Na)	4.00	5.32	6.29	7.92	9.48	5.05	7.71
An (100*Ca/(K + Ca + Na)	96.00	94.68	93.66	92.06	90.41	94.95	92.29

NOTE: Number of ions on the basis of 16 (O); total Fe is expressed as FeO*; G + ol_r gabbro with olivine; < means below detection limit

Moreover, Arculus and Wills (1980) also note that hydrous basaltic melts crystallize more anorthitic plagioclase than anhydrous melts.

Evidence for high-pressure fractionation

Several aspects of mineral compositions in the ultramafic–mafic cumulates of the Mersin ophiolite show distinct characteristics relative to low-pressure MORB-type parental magma (Dungan et al. 1978; Fisk et al. 1980; Elthon 1981). The main characteristics of low-pressure (1 atm) phase relationships are that large amounts of olivine fractionation with or without plagioclase prior to pyroxene crystallization depletes the residual liquids in MgO, the Mg# of coexisting clinopyroxene, olivine is generally low (<82) and orthopyroxene has an even lower Mg# (<74; Elthon et al. 1982). Moreover, low-pressure crystallization of MORBs would yield dunites, troctolites and olivine gabbros (Elthon et al. 1982; Pearce et al. 1984). The ultramafic rocks in the Mersin ophiolite are in contradiction with traditional low-pressure crystallization order by having dunite, wherlite, clinopyroxenite and gabbro. The high Mg# of the olivines (89.3–80), clinopyroxenes (95–77) and orthopyroxenes (77–68) in the ultramafic–mafic cumulates and high An content of plagioclase (96–90) in gabbroic rocks clearly demonstrate the incompatibility of crystallization in low-pressure MORB-type magma.

In Fig. 7 the Mg#s of coexisting olivines and clinopyroxenes are shown. It can be seen obviously that the data from the Mersin ophiolite differ from the 1-atm experiment field and overlaps with the field of high-pressure mantle xenoliths (7–10 kbar) and North Arm mountains which has been thought to have formed in a high-pressure-arc (supra-subduction) environment (Elthon et al. 1982; Elthon 1991). The high-pressure crystallization of ultramafic and mafic phases is also supported by very limited cryptic variation through 3-km-thick section (Parlak et al. 1995a).

Having unzoned and compositionally constant pyroxenes in cumulus and intercumulus minerals may indicate slow cooling in the magma chamber of the Mersin ophiolite. Flower et al. (1977) concluded that slowly cooling and unzoned minerals may occur in a high-pressure crystallization environment likely at the base of an island arc. The existence of high magnesian olivine and pyroxene and the absence of plagioclase in ultramafic rocks may suggest high pressure (ca. 10 kbar) crystallization of basaltic melt (Green and Ringwood 1967; Elthon et al. 1982; Burns 1985). This predicted high-pressure-crystallization value seems to be compatible with the Mersin ophiolite case.

Tectonic implications

It has been well documented in the study by Pearce et al. (1984) that Cretaceous ophiolites in the eastern Mediterranean, including Troodos massif, Oman, Baer Bassit (Syria), Zagros ophiolites (Iran) and ophiolitic massifs in Turkey, show arc affinity; therefore, all these massifs are so-called supra-subduction zone ophiolites (Pearce et al. 1984; Robertson 1994).

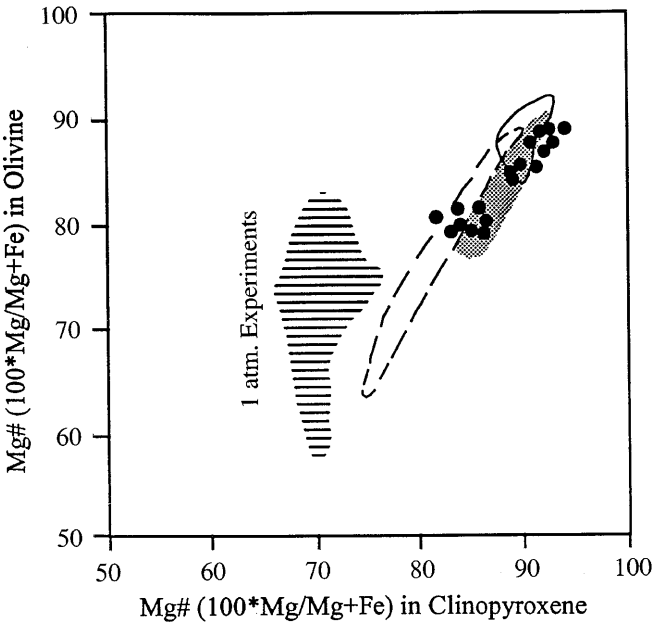

Fig. 7 Mg# (100*Mg/Mg + Fe) of coexisting olivine and clinopyroxene in the ultramafic and mafic cumulates (*filled circles*) from Mersin ophiolite. *Dashed line* represents oceanic ultramafic and mafic cumulates; *solid line* indicates high-pressure mantle xenoliths. *Shaded Dotted area* shows the Bay of Island ophiolite field. *Horizontally lined area* shows experimentally determined 1-atm phase equilibria boundaries of MORBs. The fields are after Elthon et al. (1982)

It was suggested that gabbroic rocks, occurring within an arc-like environment, differ from their oceanic equivalents in terms of their high Ca-content in plagioclase (Burns 1985). Compositions of coexisting plagioclase and clinopyroxene in the cumulate gabbros are plotted in Fig. 8a. It is clearly shown that highly calcic plagioclases and magnesian clinopyroxenes in the gabbroic rocks from the Mersin ophiolite are well correlated with arc gabbro field. Figure 8b presents the covariation of olivine and plagioclase from the Mersin, Troodos (Hébert and Laurent 1990) and other well-established tectonic settings (Hébert 1985; Beard 1986). The mineral compositions of the Mersin plutonic rocks, which present very limited fractionation in terms of An and Fo content, undoubtedly differ from the compositions of the oceanic cumulate spectrum showing high fractionation trend (Fig. 8b). The Mersin ophiolite show close similarity to particular trend of Lesser Antilles (Arculus and Wills 1980), Agrigan volcano in Mariana arc (Stern 1979) and Troodos trend, which is interpreted to have formed in an arc environment (Hébert and Laurent 1990). The major, trace and rare earth element chemistry, as well as the mineral chemistry of the basaltic rocks in the Mersin ophiolite, also suggest arc affinity (Parlak et al. 1995b). The magma chambers

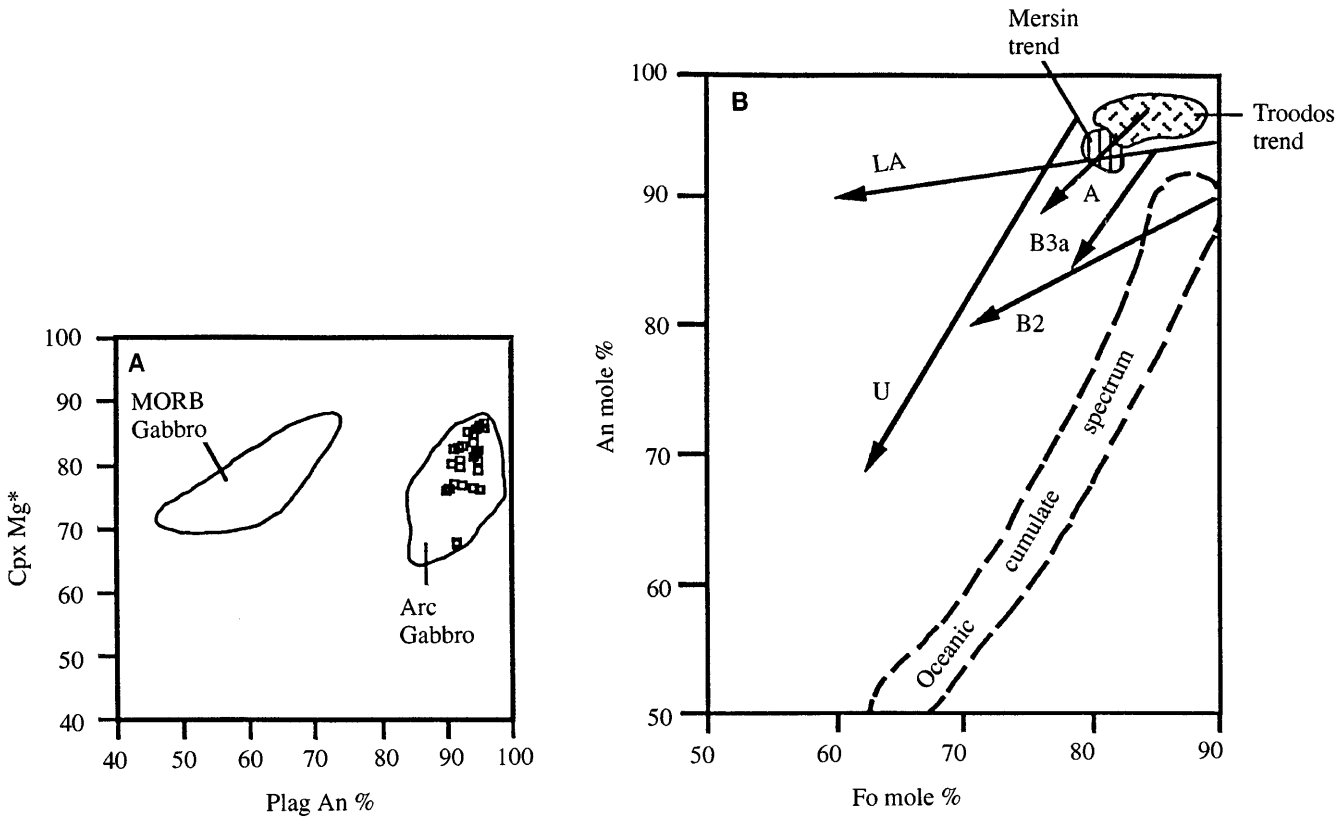

Fig. 8 **A** Composition of coexisting plagioclase and clinopyroxene in the cumulate gabbros (*squares*) from the Mersin ophiolite. Fields of MORB and arc gabbros are from Burns (1985). Note that cumulate gabbros fit well within the arc-gabbro field. **B** Covariation of olivine and plagioclase from the plutonic suite of the Mersin ophiolite and known tectonic settings (Hébert 1985; Beard 1986; Hébert and Laurent 1990). *LA* Lesser Antilles (Arculus and Wills 1980); *A* Agrigan volcano–Mariana arc (Stern 1979); *B2, B3a* Boisa volcano, Papua (Gust and Johnson 1981); *U* Usa volcano, Japan (Fujimaki 1986)

at the base of the immature arc form mafic and ultramafic cumulate sequences which crystallize at high pressures in which olivine + spinel are followed by pyroxene then plagioclase, whereas in MORB ophiolites plagioclase crystallizes before pyroxene (Burns 1985; Coleman 1986). In the plutonic suite of the Mersin ophiolite, basal dunitic layers pass into wherlites and clinopyroxenites which show the same conditions as at the base of island-arc magma chambers as in Border Range ultramafic and mafic complex (Burns 1985).

Conclusions

The following conclusions were reached as a result of this work:

1. Major and trace element geochemistry of the ultramafic and mafic cumulates suggest an arc-like tectonic environment for the generation of the Mersin ophiolite oceanic lithosphere. This data is well correlated with the geochemistry of the co-genetic basaltic units which indicates also arc-like/supra-subduction-zone tectonic environment.
2. Mineral chemistry of ultramafic and mafic cumulates indicates high-pressure (ca. 10 kbar) crystallization from a basaltic melt. This evidence is based on the crystallization order of the cumulus and intercumulus minerals (Olivine ± chromian spinel + clinopyroxene + plagioclase and orthopyroxene), absence of plagioclase in the ultramafic rocks, presence of Ca-rich plagioclase (An_{95-91}) and highly magnesian olivine (Fo_{91-80})–clinopyroxene ($Mg\#_{95-77}$).
3. Petrological, mineralogical and field evidences suggest the following evolutionary scenario for the Mersin ophiolite: opening of the South Atlantic around Early–Late Cretaceous (Smith et al. 1981); compressional regime started between Afro-Arabia and Eurasia in the eastern Mediterranean region; north-dipping subduction of the southern segment of the Neo-Tethyan ocean started during Mid-Cretaceous (Sengör and Yılmaz 1981; Aktas and Robertson 1984; Dilek and Moores 1990). The Mersin ophiolite formed above this intra-oceanic subduction zone some time at the beginning of Late Cretaceous. Soon after the formation of the oceanic lithosphere, the Mersin ophiolite was emplaced onto the Tauride active continental margin during the end of Late Cretaceous–Early Palaeocene time. Neo-autochthonous sediments, Late Palaeocene in age, cap ophiolite body with angular unconformity indicating cessation of the ophiolite obduction in the study area (Avsar 1992).

Acknowledgements This was a part of the Ph.D. study of O. Parlak supported by Swiss National Science Foundation (grant no. 2000–40240.94/1). We are grateful to Fabio Capponi and Michèle Senn-Gerber for major and trace element analyses. Dr. A. A. Gurenko and an anonymous reviewer critically read the manuscript and made important suggestions for its improvement. Thanks are due to Ö. Faruk Çelìk and Alican Kop for their assistance in the field. We acknowledge T. Feeley and F. Bussy for their guidance during the microprobe analyses at Lausanne University.

References

Aktas G, Robertson AHF (1984) The Maden complex, SE Turkey: evolution of a Neotethyan active margin. Geol Soc Spec Publ 17:375–403

Aoki K, Kushiro I (1968) Some clinopyroxenes from ultramafic inclusions in Dreiser Weiher, Eifel. Contrib Mineral Petrol 21:743–749

Arculus RJ, Wills KJA (1980) The petrology of plutonic blocks and inclusions from the Lesser Antilles island arc. J Petrol 21:743–99

Avsar N (1992) Namrun (Icel) yoresi Paleojen bentik foraminifer faunasi. MTA dergisi 114:127–144

Bari SM de, Coleman RG (1986) Petrologic aspects of gabbros from the Tosnia complex, Chugach mountains, Alaska: evidence for deep magma chambers under an island arc. Geol Soc Am (abstracts and programs) 18:99

Bari SM de, Coleman RG (1989) Examination of the deep levels of an island arc: evidence from the Tonsina ultramafic–mafic assemblage, Tonsina, Alaska. J Geophys Res 94:4373–4391

Bari SM de, Kay SM, Kay, RW (1987) Ultramafic xenoliths from Adagdak Volcano, Adak, Aleutian islands, Alaska: deformed igneous cumulates from the moho of an island arc. J Geol 95:329–41

Beard JS (1986) Characteristic mineralogy of arc-related cumulate gabbros: implications for the tectonic setting of gabbroic plutons and for andesite genesis. Geology 14:848–851

Brown GC (1982) Calc-alkaline intrusive rocks: their diversity, evolution and relation to volcanic rocks. In: Thorpe RS (ed) Andesites: orogenic andesites and related rocks. Wiley, New York, pp 437–461

Burns LE (1985) The Border Ranges ultramafic and mafic complex, south-central Alaska: cumulate fractionates of island-arc volcanics. Can J Earth Sci 22:1020–1038

Coish RA, Taylor LA (1979) The effects of cooling rate on texture and pyroxene chemistry in DSDP leg 34 basalt: a microprobe study. Earth Planet Sci Lett 42:389–398

Coleman RG (1986) Ophiolites and accretion of the North American Cordillera. Bull Soc Geol France 8:961–968

Conrad WC, Kay RW (1984) Ultramafic and mafic inclusions from Adak island: crystallization history and implications for the nature of primary magmas and crustal evolution in the Aleutian arc. J Petrol 25:88–125

Dick HJB, Bullen T (1984) Chromium spinel as a petrogenetic indicator in abyssal and alpine-type peridotites and spatially associated lavas. Contrib Mineral Petrol 86:54–76

Dilek Y, Moores EM (1990) Regional tectonics of the eastern Mediterranean ophiolites. In: Malpas J, Moores E, Panayiotou A, Xenophontos C (eds) Ophiolites-oceanic crustal analogues. Proc Troodos Ophiolite Symp 1987, pp 295–309

Dungan MA, Long PE, Rhodes JM (1978) The petrology, mineral chemistry, and one atmosphere phase relations of basalts from site 395. Init Rep Deep Sea Drill Project 45:461–472

Dupuy C, Dostal J, Marcelot G, Bougault H, Joron JL, Treuil M (1982) Geochemistry of basalts from central and southern New Hebrides arcs: implication for their source rock composition. Earth Planet Sci Lett 60:207–225

Elthon D (1981) 1 atm phase equilibria of basalts from the Tortuga ophiolite complex, with implications for magma chamber processes. Chapman Conference on the Generation of the Oceanic Lithosphere-AGU

Elthon D (1987) Petrology of gabbroic rocks from the Mid-Cayman rise spreading center. J Geophys Res 92:658–682

Elthon D (1991) Geochemical evidence for formation of the Bay of Island ophiolite above subduction zone. Nature 354:140–143

Elthon D, Casey JF, Komor S (1982) Mineral chemistry of ultramafic cumulates from the North Arm Mountain massif of the Bay of Islands ophiolite: evidence for high-pressure crystal fractionation of oceanic basalts. J Geophys Res 87:8717–8734

Elthon D, Casey JF, Komor S (1984) Cryptic mineral chemistry variations in a detailed traverse through the cumulate ultramafic rocks of the North Arm Mountain massif of the Bay of Island ophiolite, Newfoundland. Geol Soc Lond Spec Publ 13:83–97

Fisk MR, Schilling JG, Sigurdsoon H (1980) An experimental investigation of Iceland and Reykjanes Ridge tholeiites. I. Phase relations. Contrib Mineral Petrol 74:361–374

Flower MFJ, Robinson PT, Schmincke HU, Ohnmacht W (1977) Magma fractionation systems beneath the Mid-Atlantic ridge at 36–37°N. Contrib Mineral Petrol 64:167–195

Fujimaki H (1986) Fractional crystallization of the basaltic suite of Usu volcano, southwest Hokkaido, Japan, and its relationships with the associated felsic suite. Lithos 19:129–140

Gamble RP, Taylor LA (1980) Crystal/liquid partitioning in augite: effects of cooling rate. Earth Planet Sci Lett 47:21–33

Green TH, Ringwood AE (1967) Genesis of basaltic magmas. Contrib Mineral Petrol 15:103–190

Gust DA, Johnson RW (1981) Amphibole bearing cumulates from Boisa island, Papua New Guinea: evaluation of the role of fractional crystallization in an andesitic volcano. J Geol 89:219–232

Hébert R (1982) Petrography and mineralogy of oceanic peridotites and gabbros: some comparisons with ophiolite examples. Ofioliti 7:299–324

Hébert R (1985) Pétrologie des roches ignées océaniques et comparison avec les complexs ophiolitiques du Québec, de Chypre et de L'Apennin: Thèse d'Etat, Université de Bretagne Occidentale, Brest, 542 pp

Hébert R, Laurent R (1990) Mineral chemistry of the plutonic section of the Troodos ophiolite: new constraints for genesis of arc-related ophiolites. In: Malpas J, Moores E, Panayiotou A, Xenophontos C (eds) Ophiolites–oceanic crustal analogues. Proc Troodos Ophiolite Symp 1987, pp 149–163

Hodges FN, Papike JJ (1976) DSDP site 334: magmatic cumulates from ocean layer 3. J Geophys Res 81:4135–4151

Irvine TN (1967) Chromian spinel as a petrogenetic indicator. Part 2. Petrologic applications. Can J Earth Sci 4:71–103

Jaques AL, Chappell BW, Taylor SR (1983) Geochemistry of cumulus peridotites and gabbros from the Marum ophiolite complex, northern Papua New Guinea. Contrib Mineral Petrol 82:154–164

Johannes M (1978) Melting of plagioclase in the system Ab–An–H_2O at $PH_2O = 5$ kbar, an equilibrium problem. Contrib Mineral Petrol 66:295–303

Juteau T (1980) Ophiolites of Turkey. Ofioliti 2:199–238

Komor SC, Elthon D, Casey JF (1985) Mineralogical variations in layered ultramafic cumulate sequences at the North Arm Mountain massif, Bay of Island ophiolite, Newfoundland. J Geophys Res 90:7705–7736

Komor SC, Elthon D, Casey JF (1986) Petrology of layered gabbroic rocks from the North Arm Mountain massif, Newfoundland. Contrib Mineral Petrol

Medaris LG (1972) High pressure peridotites from in south-western Oregon. Geol Soc Am Bull 83:41–58

Pallister JS, Hopson CA (1981) Samail ophiolite plutonic suite: field relations, phase variation, cryptic variation and layering and a model of a spreading ridge magma chamber. J Geophys Res 86:2593–2644

Parlak O, Delaloye M, Bingöl E (1995a) Magma chamber process in Mersin ophiolite, S. Turkey. Abstracts of Int Ophiolite Symp, 18–23 September, Pavia, Italy, 109 pp

Parlak O, Delaloye M, Bingöl E (1995b) Geochemistry and tectonic setting of volcanic rocks in Mersin ophiolite, S. Turkey. Abstracts of Int Earth Sci Colloquium on the Aegean Region (IESCA-95), 9–14 October, Izmir (Güllük), Turkey, 43 pp

Pearce JA, Norry MJ (1979) Petrogenetic implications of Ti, Zr, Y and Nb variations in volcanic rocks. Contrib Mineral Petrol 69:33–47

Pearce JA, Lippard SJ, Roberts S (1984) Characteristics and tectonic significance of supra-subduction zone ophiolites. In: Kokelaar BP, Howells MF (eds) Marginal basin geology. Blackwell, Oxford, pp 77–94

Ricou LE (1971) Le croissant ophiolitique péri-arabe, une ceinture de nappes meses en place au Crétacé supérieur. Rev Géog Phys Géol Dyn 13:327–349

Robertson AHF (1994) Role of the tectonic facies concept in orogenic analysis and its application to Tethys in the eastern Mediterranean region. Earth Sci Rev 37:139–213

Ross M, Huebner JS (1975) A pyroxene geothermometer based on composition–temperature relationships of naturally occurring orthopyroxene, pigeonite and augite. In: Extended Abstracts of the Int Conference of Geothermometry and Geobarometry, Pennsylvania State University, University Park, Pennsylvania, 4 pp

Sengör AMC, Yilmaz Y (1981) Tethyan evolution of Turkey: plate tectonic approach. Tectonophysics 75:181–241

Shervais JW (1990) Island arc and oceanic crust ophiolites: contrasts in the petrology, geochemistry and tectonic style of ophiolite assemblages in the California Coast ranges. In: Malpas J, Moores E, Panayiotou A, Xenophontos C (eds) Ophiolites–oceanic crustal analogues. Proc Troodos Ophiolite Symposium 1987, pp 507–520

Smith AG, Hurley AM, Briden JC (1981) Phanerozoic palaeocontinental maps. Cambridge University Press, Cambridge, p. 102

Smith TE, Huang CH, Wallawender MJ, Cheung P, Wheeler C (1983) The gabbroic rocks of the Peninsular Ranges Batholiths, southern California: cumulate rocks associated with calc-alkalic basalts and andesites. J Volcan Geotherm Res 18:249–278

Stern RJ (1979) On the origin of andesite in the northern Mariana island arc: implications from agrigan. Contrib Mineral Petrol 68:207–219

Streckeisen A (1976) To each plutonic rock its proper name. Earth Sci Rev 12:1-33

Yalınız MK, Göncüoglu MC, Floyd PA (1994) Geochemical characteristics and geodynamic interpretation of the Supra-subduction Sarıkaman ophiolite, Central Anatolia. Abstracts of Int Volcanological Congr (IAVCEI-94) 12–16 September, Ankara, Turkey, 162 pp